Ex Situ CdSe Quantum Dot–Sensitized Solar Cells Employing Inorganic Ligand Exchange To Boost Efficiency

ARTICLE *in* THE JOURNAL OF PHYSICAL CHEMISTRY C · JANUARY 2014

Impact Factor: 4.77 · DOI: 10.1021/jp410599q

THE JOURNAL OF PHYSICAL CHEMISTRY C

Article

pubs.acs.org/JPCC

Ex Situ CdSe Quantum Dot-Sensitized Solar Cells Employing Inorganic Ligand Exchange To Boost Efficiency

Feng Liu,[†] Jun Zhu,*[,†] Junfeng Wei,[†] Yi Li,[†] Linhua Hu,[†] Yang Huang,[†] Oshima Takuya,[‡] Qing Shen,*[,‡,§] Taro Toyoda,[‡,§] Bing Zhang,[∥] Jianxi Yao,[∥] and Songyuan Dai*[,†,∥]

[†]Key Laboratory of Novel Thin Film Solar Cells, Institute of Plasma Physics, Chinese Academy of Sciences, P.O. Box 1126, Hefei, Anhui 230031, People's Republic of China

[‡]Department of Engineering Science, Faculty of Informatics and Engineering, The University of Electro-Communications, 1-5-1 Chofugaoka, Chofu, Tokyo 182-8585, Japan

[§]CREST, Japan Science and Technology Agency (JST), 4-1-8 Honcho, Kawaguchi, Saitama 332-0012, Japan

[∥]School of Renewable Energy, North China Electric Power University, Beijing 102206, People's Republic of China

Supporting Information

ABSTRACT: We present an effective way to boost the as-synthesized CdSe quantum dot-sensitized solar cells (QDSSCs) performance by introducing an inorganic ligand exchange strategy into this traditional system. Inorganic ligand exchange, to the best of our knowledge, is designed for the first time for CdSe-based QDSSCs, and it features low-cost, easy operation, and repeatable process. The route involves the direct deposition of the CdSe quantum dots (QDs), which were initially capped with trioctylphosphine (TOP) ligands onto mesoporous TiO_2 nanocrystalline electrodes and followed by a post-treatment of the sensitized photoanode films with sulfur ions (S^{2-}) solution. Here, changes in surface chemical status of CdSe QDs during the inorganic ligand exchange process and the influence of ligand exchange on the electron's ultralfast transfer between nanoparticles were investigated through XPS and femtosecond transient grating techniques, respectively. With the inorganic ligand passivated CdSe QDs, the QDSSCs exhibited a power conversion efficiency of 3.17% (AM1.5G, 100 mW/cm^2), 65% higher than that of the organic ligands capped QDSSCs.

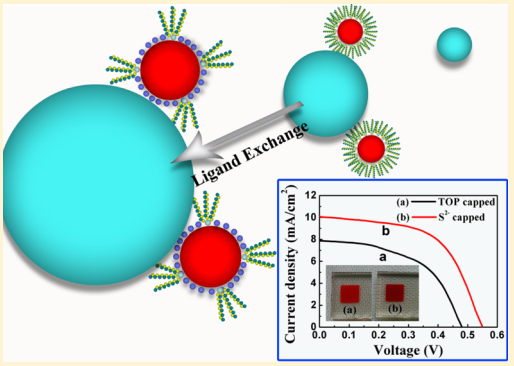

INTRODUCTION

Quantum dot-sensitized solar cells are gaining more attention as they show great promise toward the development of the next generation solar cells.[1−4] QDs, the photosensitizer, such as CdS,[5] CdSe,[6] PbS,[7] PbSe,[8] Sb_2S_3,[9] organic−inorganic perovskite,[10,11] etc., with their size-dependent band gap can be used to match the solar spectrum, providing new opportunities for boosting the power conversion efficiency (PCE) of solar cells.

Up to now, two major methods have been employed to deposit QDs onto wide gap nanostructured semiconductor electrodes such as TiO_2, SnO_2, and ZnO for photoanode sensitization: in situ and ex situ. Generally, in situ approaches such as chemical bath deposition (CBD) and successive ionic layer adhesion and reaction (SILAR) allow QDSSCs to give a relatively higher efficiency. These approaches, however, allow little control over the size and shape of the deposited QDs. Use of the presynthesized QDs as sensitizers in the alternative approach of the ex situ method can avoid the above shortcoming, whereas they have frequently been reported with lower PCE.

For QDSSCs prepared by the ex situ method, some efforts have been devoted and PCE improved when the initial long carbon chain organic capping ligands were replaced with shorter ones. For example, such ligand exchange has been carried out by Grätzel's group in which the initial TOPO/TOP ligands of CdSe QDs were replaced with the shorter pyridine passivants to facilitate charge transfer, resulting in a PCE of 1.0% for CdSe QDSSCs with cobalt(II/III)-based electrolyte.[12] More recently, Zhong's group employed mercaptopropionic acid to replace the original organic passivants oleylamine/TOP of CdSe, $CdSe_xTe_{1-x}$ alloyed QDs, core/shell CdS/CdSe, and CdTe/CdSe QDs, and achieved high PCE.[13−16] However, density functional theory (DFT) used by Sargent's group has demonstrated that the steric considerations prevent these organic ligands from infiltrating the hard-to-access trenches on the surface of QDs, causing unpassivated metal surface sites to remain.[17] This kind of drawback caused by organic ligands can be overcame by utilizing the inorganic single-atom capping layer instead. In depleted PbS QD heterojunction and homojunction solar cells, some efforts have been made in this way aimed at improving the passivation of surface defects to decrease recombination loss and enhance electron transport

Received: October 27, 2013
Revised: December 11, 2013
Published: December 18, 2013

between nanocrystals.[18,19] Unfortunately, there have been few studies on inorganic ligands capped ex situ QDSSCs up to now.[20,21] The first reason is the inorganic ligand exchanging procedure designed for colloidal QD films cannot be extended to QDs deposited on mesoporous films. The second reason is the present inorganic ligand exchanging method mainly focused on PbS QDs with initial carboxyl group-based ligands (such as oleic acid ligands used in Sargent's group), while the most frequently used CdSe QDs in the ex situ prepared QDSSCs are usually capped by TOP or TOPO ligands.

Here, we developed a simple inorganic ligand exchange route that takes advantage of the small size of sulfur ions, as well as the mutual binding affinity between sulfur and cadmium to passivate the CdSe QDs and to increase short-range interparticles' communication between QDs and TiO_2 nanocrystals. This process was defined as S^{2-} ligand exchange. We found this inorganic ligand exchange has led to an impressive improvement in cells' performance. Although the PCE of 3.17% we achieved was less competitive when compared to the typical dye-sensitized solar cells, the main point lies in providing new insights into the role of the inorganic ligands and giving more opportunities to boost the efficiency of the QDSSCs and those organic ligands-based quantum dot solar cells. In general, it helps us to recognize the enormous potential of exploiting the ex situ method for depositing the presynthesized QDs onto TiO_2 mesoporous films and highlights the importance of surface modification that intended to improve the passivation of surface defects and facilitate electron injection from QDs to TiO_2 nanocrystals.

EXPERIMENTAL DETAILS

Chemicals for QD Preparation. Oleic acid (OA) (tech. grade, 90%), cadmium nitrate tetrahydrate (99.9% metal basis), and selenium powder (−100 mesh, 99.999%) were purchased from Alfa Aesar. Technical grade trioctylphosphine (TOP) (97%) was purchased from Aldrich Chemicals. Myristic acid was purchased from URChem (99%, China). Sodium sulfide nonahydrate (≥98.0%) was obtained from Sinopharm Chemical Reagent Co., Ltd. Selenium oxide (99.8%) was from Acros Organics (Pittsburgh, PA). Sodium borohydride (98%) was obtained from J&K Chemical Ltd. All of the chemical reagents were used as received.

Preparation of Cadmium Myristate. Cadmium myristate as the precursor of cadmium was prepared using a modified recipe described before.[22] Cadmium nitrate tetrahydrate (0.5 mmol, 0.1542 g) was dissolved in 5 mL of anhydrous methanol. Sodium hydroxide (1.5 mmol) and myristic acid (1.5 mmol) were dissolved in 50 mL of anhydrous methanol with vigorous stirring at room temperature, resulting in the sodium myristate solution. Next, the cadmium nitrate solution was added dropwise into the sodium myristate solution. Finally, the resulting white precipate was washed with anhydrous methanol three times, and then dried at 50 °C under vacuum overnight to remove the residual methanol.

Synthesis of CdSe QDs. CdSe QDs dispersed in chloroform were synthesized on the basis of the method developed by Wang et al.,[23] and it was noted that QDs prepared in this way were initially TOP capped.[24,25] Briefly, in a sealed autoclave, 0.05 mmol of selenium powders reacts with 0.1 mmol of cadmium myristate in toluene in the presence of TOP and OA. The reaction temperature was settled at 180 °C, and an appropriate reaction time was chosen for particles' growth. After the synthesis, the nanocrystals were precipitated with methanol, and then washed by repeated redissolution in toluene and precipitation with addition of methanol. This precipitation cycle was performed two or three times, and the QDs were finally dissolved in chloroform, with excess ligands and organic species being removed. The optical property and TEM image of the resulting CdSe QDs are presented in Supporting Information 1.

Fabrication of QDs-Sensitized Photoanodes. TiO_2 mesoporous electrodes with a light-scattering layer were prepared according to our previous report,[26] and the whole thickness of the TiO_2 photoelectrodes used here was around 17 μm including the light-scattering layer with the thickness of 8 μm. QDs-sensitized photoanodes were obtained by directly immersing the films into CdSe QDs chloroform dispersion (~2.5 mM) in open air under ambient conditions and maintaining for 72 h before being rinsed with chloroform and ethanol and then dried with nitrogen. The prepared sensitized films were stored in a vacuum atmosphere for further use. More details about QDs' adsorption onto TiO_2 films are presented in Supporting Information 2.

Post-Treatment of the Sulfur Ions Solution (S^{2-} Ligand Exchange). S^{2-} ligand exchange was carried out as follows: the CdSe QDs-sensitized TiO_2 mesoporous films were immersed into a mixture solution of sodium sulphide (Na_2S) in water/methanol (volume ratio of 1:1) with the concentration of 0.08 M for 46 h under dark conditions. The treated films then were washed sequentially with water and methanol and finally dried in air conditions.

ZnS Layer. After the QDs' deposition and post-treatment of sulfur ions were finished, photoanodes were dipped alternately into 0.1 M $Zn(NO_3)_2$ ethanol solution and 0.1 M Na_2S methanol solution for 1 min/dip to form a ZnS buffer layer; each dip process was followed by a rinse with the corresponding solvent and drying in air. The above procedure is defined as one SILAR cycle, and two cycles of ZnS were carried out in this study.

Preparation of Cu_2S Counter Electrode. The counter electrodes of QDSSCs used here were brass foils supported Cu_2S films prepared on the basis of Hodes et al.'s method.[27] Typically, the polished brass foils were immersed in HCl (37%) solution at 70 °C for 5 min and subsequently washed with water, which was then followed by sulfidation in the prepared polysulfide solution.

Polysulfide Electrolyte Solution and Assembling of Solar Cells. The polysulfide electrolyte solution consists of 1.0 M Na_2S, 1.0 M S, and 0.1 M NaOH in 5 mL of deionized water solution. The solar cells were assembled by sandwiching the photoanode and the Cu_2S-coated counter electrode using a thermal adhesive film (Surlyn, 60 μm, Dupont). The polysulfide electrolyte solution then was injected by vacuum backfilling followed by the sealing process using a Surlyn film and a cover glass. The active area of the mask covered solar cells was measured to be 0.25 cm^2.

Characterization. UV−vis absorption spectra were obtained by using a spectrophotometer (HITACHI, U-3900H, Japan). HR-TEM images were recorded by a JEM-2010 (JEOL, Japan) high-resolution transmission electron microscope. X-ray powder diffraction (XRD) spectra were taken on an X-ray diffraction analysis instrument (TTR-III, Rigaku Corp., Japan) with Cu Kα irradiation (λ = 0.1541 nm). Fourier transform-infrared spectroscopy (FT-IR) was measured with a Nicolet 8700 (U.S.) FTIR spectrometer. A typical EDS spectrum was performed with an energy dispersive spectrometer equipped on

dx.doi.org/10.1021/jp410599q | J. Phys. Chem. C 2014, 118, 214−222

the TEM equipment. Elemental analysis of CHS was conducted using an Elementar vario EL cube. X-ray photoelectron spectroscopy (XPS) data were accumulated on an ESCA-LAB250 XPS system (Thermo, U.S.). An improved transient grating (TG) technique[28−38] (it was also called lens-free heterodyne detection transient grating (LF-HD-TG) technique in some previous papers) was used to characterize ultrafast carrier dynamics to reveal factors concerning the injection process. The principle and setup of the improved TG technique have been described in previous papers.[28−38] The TG method monitors the change in the refractive index of the sample upon photoexcitation. In this experiment, the laser source was a titanium/sapphire laser (CPA-2010, Clark-MXR Inc.) with a wavelength of 775 nm, a repetition rate of 1 kHz, and a pulse width of 150 fs. The light was separated into two parts. One-half of it was used as a probe pulse. The other half of the light was used to pump an optical parametric amplifier (OPA) (a TOAPS from Quantronix) to generate light pulses with a wavelength tunable from 290 nm to 3 μm, used as a pump light in the TG measurement. In this study, the experiment was carried out under N_2 environment, and under excitation wavelength of 520 nm. Upon this excitation wavelength, the optical absorption of the anatase TiO_2 electrode is negligible, and the TG signals can be considered to result from the optical absorption of the CdSe QDs. The probe light wavelength is 775 nm. The typical laser pulse intensity used in the TG experiments was as low as 2 mW (2 μJ/pulse and the repetition frequency of the laser pulse is 1 kHz), although in some experiments it was increased to 20 mW. The area of the laser beam on the sample was about 0.2 cm^2. Therefore, the typical pump light intensity was as low as 10 mW cm^{-2}. The samples showed no apparent photodamage during the TG measurements. Incident photon-to-current efficiency (IPCE) curves were operated with a QE/IPCE measurement kit (Newport, U.S.) using a 300 W Xe lamp and a monochromator. Electrochemical impedance spectroscopy (EIS) measurements were investigated with a FRA equipped PGSTAT-30 from Autolab (AUT302N, Metrohm, Switzerland). $J-V$ characteristics of QDSSCs were derived with a Keithley 2420 digital source meter (Keithley, U.S.) under a 450 W xenon lamp (Oriel Sol3A Solar Simulator 94043, Newport Stratford Inc., U.S.).

RESULTS AND DISCUSSION

Optical Property. We first took a closer inspection of the UV−vis absorption spectra of the CdSe QD solution and CdSe QDs-sensitized TiO_2 films. As shown in Figure 1a, the sharp exciton absorption peak at 575 nm of the CdSe QDs dispersion in chloroform solvent reveals the mean particle size of 3.5 nm and a narrow size distribution.[24,39] When the QDs were adsorbed on TiO_2 films, there is a blue-shift in the exciton absorption peak (Figure 1b). Such a blue-shift that occurred when incorporating the QDs into the TiO_2 matrix was also observed by Guijiarro et al.[24] An additional explanation here can be the reduction in CdSe QDs diameter by the loss of a certain layer of initial CdSe to oxidation. In fact, the peak at around 59.2 eV was observed in XPS spectra, indicating the presence of SeO_2 on the surface of QD. It is noted that after S^{2-} ligand exchange, the absorption peak exhibited a red-shift (20 nm) (Figure 1c, dotted line). We had initially suspected this small red-shift to be attributed to the formation of $CdSe_xS_{1-x}$ external to the CdSe QDs, which features a narrower band gap with respect to the parent CdSe nanoparticles.[40]

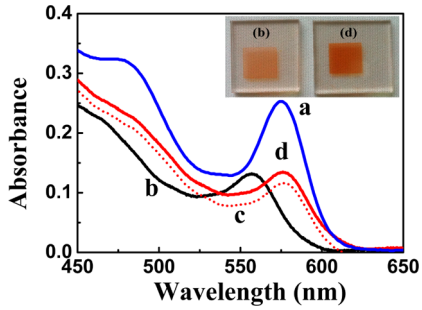

Figure 1. UV−vis absorption spectra: (a) CdSe QD dispersion in chloroform, (b) CdSe QDs on TiO_2 films, (c) CdSe QDs on TiO_2 films after S^{2-} ligand exchange (dotted line), and (d) CdSe QDs on TiO_2 films after a modified ligand exchange procedure. Thickness of the TiO_2 films without scattering layer used here for UV−vis spectra was about 3 μm.

Chakrapani et al. have pointed out that such a ternary compound may exist when CdSe QDs undergo photoanodic corrosion in Na_2S electrolyte under visible irradiation.[40] Things were different in our case in that the S^{2-} ligand exchange process was carried out under dark conditions. Moreover, XRD patterns of the CdSe QDs did not show any change after ligand exchange (see Supporting Information Figure S3). Therefore, the formation of such a ternary compound could be ruled out. We believe that the observed red-shift is related to the change of surface ligands around the QDs, which would induce a redistribution of electronic density in QDs. As described in Koole et al.'s report,[41] a similar red-shift after ligand exchange was observed, and they attributed the shift to the effect of thiol groups (−SH) attaching to the Cd-terminated CdSe nanocrystal surface, forming a stronger new Cd−thiol bond that influences the electronic structure of the CdSe QDs. In fact, Talapin et al.[42] have also verified the surface ligands-related shift in CdSe QDs.

A decrease in absorption intensity of the TiO_2/CdSe film can be observed after S^{2-} treatment, indicating the desorption process of QDs from TiO_2 occurred. It is worthy mentioning that the attachment of QDs to TiO_2 matrix is driven by an equilibrium and desorption promoted if the Na_2S solution was initially fresh. Such QDs' desorption would be adverse in consideration of light harvesting. Therefore, we modified this ligand exchange process by adding a very small amount of CdSe QDs, which had been transferred to the aqueous phase[43] to S^{2-} solution (the final concentration of the water-soluble CdSe QDs that added to S^{2-} solution was 0.03 mM) and successfully retained the absorption intensity as untreated film (Figure 1d).

FT-IR Spectra. We further inspected the organic composition of the photoanode films before and after S^{2-} ligand exchange. The FTIR spectra show visibly that the symmetrical and asymmetrical stretching vibrations of C−H signal peak intensity at 2853 and 2923 cm^{-1}, which come from the TOP alkyl chain, are much reduced after S^{2-} ligand exchange. In addition, the broad peak at 1000−1145 cm^{-1} in Figure 2b, which is assigned to TOP's absorption, also almost disappeared, a strong evidence that the initial TOP ligands were mostly removed from the particle surface after ligand exchange (Supporting Information Figure S4 confirms the FTIR spectra of TOP). The removal of TOP ligands can be explained in that most of the TOP ligands are not strongly bound to CdSe QDs' surface (the interaction between TOP ligands and QDs will be further discussed in XPS Analysis).[44]

dx.doi.org/10.1021/jp410599q | J. Phys. Chem. C 2014, 118, 214−222

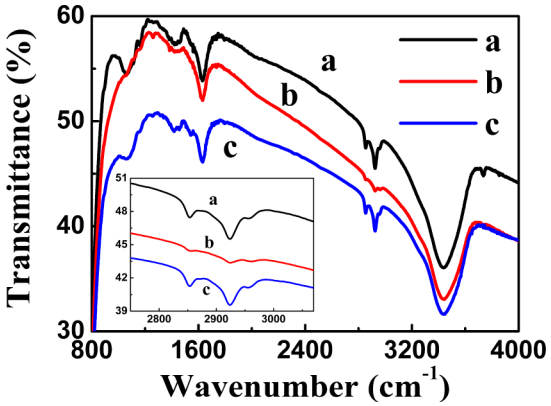

Figure 2. FTIR spectra: (a) TiO_2/CdSe film of untreated, (b) TiO_2/CdSe film after S^{2-} ligand exchange, and (c) TiO_2/CdSe film of water and methanol mixture solvent treated.

The mere immersion of the CdSe QDs-sensitized TiO_2 films into water and methanol mixture solvent without any S^{2-} at the same time was not found to have the organic ligands decreased (Figure 2c), and we did not see any improvement in the cells' performance either, thus highlighting the important role that the sulfur ions played in the ligand exchange process with the initial TOP ligands.

EDS Results. The energy dispersed spectroscopy (EDS) of the TiO_2/CdSe films before and after S^{2-} ligand exchange is presented in Figure 3. Cu peaks in all spectra come from the

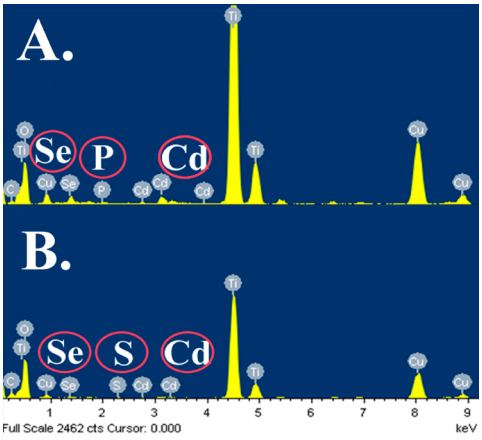

Figure 3. Typical energy dispersed spectroscopy (EDS) spectra of the CdSe QDs-sensitized TiO_2 films: (A) before and (B) after S^{2-} ligand exchange.

TEM grid, P signal peak in Figure 3A results from the TOP ligands, C peak mainly originates from the TEM carbon supporting film and partially from the TOP ligands, and Ti and O peaks are from the TiO_2 nanoparticles. S peaks appeared only after the ligand exchange procedure, as we can see from Figure 3B, confirming that the sulfur ions have been successfully incorporated into the QDs. We have ruled out the probability that the detected S signal came from the TiO_2 films, described in Supporting Information 5. The P signal that results from TOP ligands almost disappears with the present detection limit after the ligand exchange prodecure, also indicating that the TOP ligands were lost to a large degree. Quantitative analysis of the EDS spectra (Table 1) shows that the atomic ratio of Se and Cd decreased after ligand exchange. We believe it was associated with the loss of surface ligands as described in XPS Analysis. So far, we have made it clear that the S^{2-} treatment involves the decrease in TOP ligands and the introduction of S^{2-} onto the QDs' surface to replace as the new surface ligands in terms of S^{2-} ligand exchange.

Elemental Analysis of CHS. The elemental analysis of CHS in TiO_2/CdSe films was performed to characterize the contents of C, H, and S. Given the low percentage of C, H, and S contents in TiO_2/CdSe films, the influencing factors such as environmental contamination cannot be ignored. Yet we suppose the influencing factors in both samples are basically identical as they were prepared under the same ambient condition. Therefore, changes of the C and H contents could reflect to a certain extent the change of the organic ligands in QDs. As we can see from Table 2, the detected C and H elements decreased and S element appeared in the treated sample. It is consistent with the analysis in EDS spectra, thus further confirming the removal of TOP ligands and introduction of S^{2-} into QDs during the S^{2-} ligand exchange procedure.

Table 2. Elemental Analysis (Weight %) of the TiO_2/CdSe Films

sample	sample weight (mg)	C% (±0.3%)	H% (±0.3%)	S% (±0.5%)
untreated	1.961	0.90	0.52	0.00
S^{2-} treated	1.893	0.37	0.34	1.27

XPS Analysis. TOP ligands exist on the surface of CdSe QDs mainly in the form of TOPSe and bind to Cd atoms through the selenium atom.[45−47] A question should be answered that in what form do the incoming S^{2-} ligands exist on the surface of QDs. X-ray photoelectron spectroscopy (XPS) measurement was used, on one hand, to observe the composition of QDs (but we failed to give the accurate measured value of P due to the interference signal from the Se Auger peak at 134−135 eV[44]), and, on the other hand, as a sensitive way to detect the binding energy (BE) that could be indicative of a slight change in chemical status of a certain element. In Figure 4A, the BE peaks of the untreated sample at 405.4 and 412.1 eV are assigned to Cd $3d_{5/2}$ and Cd $3d_{3/2}$, which show good agreement with the reported value of CdSe,[48] while the peaks of Cd $3d_{5/2}$ and Cd $3d_{3/2}$ moved slightly toward the lower BE (ca. 0.3 eV) when the films were subjected to immersion into Na_2S solution. This implies that the surface chemical status of Cd atoms changed somewhat after ligand exchange with respect to that of the untreated. We attribute this change as arising from the treating procedure in which the sulfur ions were introduced onto the CdSe QDs' surface and meanwhile replacing the TOPSe ligands, which were initially

Table 1. Quantitative Atomic % Analysis of EDS Spectra

sample	%C	%Cu	%Ti	%O	%Cd	%Se	%P	%S
untreated	12.78	2.36	24.98	58.97	0.34	0.26	0.31	0
S^{2-} treated	13.78	2.52	20.63	62.29	0.31	0.15	0.09	0.23

dx.doi.org/10.1021/jp410599q | J. Phys. Chem. C 2014, 118, 214−222

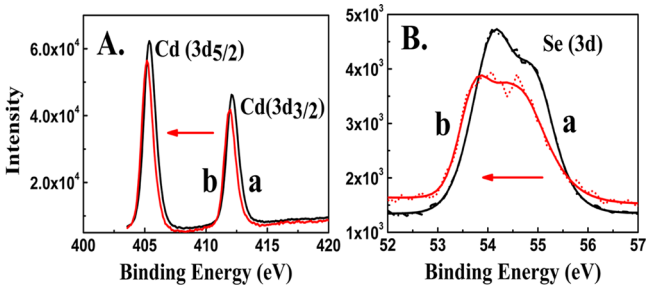

Figure 4. X-ray photoelectron spectroscopy (XPS) of Cd 3d (A), and Se 3d (B): (a) before and (b) after S^{2-} ligand exchange of the CdSe QDs-sensitized TiO_2 films. C 1s binding energy at 285.0 eV of contaminant carbon was used as an internal reference.

bound to Cd atoms to form a strong new S−Cd bond. In fact, it is been reported that in TOPO-capped CdSe QDs, the initial TOPO ligands, which had mainly interacted with the Cd atoms, could be replaced by the thiol functional groups (−SH)-containing ligands via this very deprotonated thiol group to complex with the Cd atoms on the surface of CdSe nanocrystals, forming a strong thiol adsorption through the −S−Cd structure.[49,50] In addition, Liu et al. had also observed the same tendency that the BE of Cd 3d slightly decreased (~0.3 eV) when the TOPO capping ligands were replaced with thiol molecules and formed the −S−Cd bonding type.[50] The Se 3d peak position in Figure 4B also changed with the normal distribution center decreased in the treated film (from ~54.5 to ~54.3 eV). We believe that the BE of Se 3d in CdSe nanocrystals is mainly determined by the Se−Cd bond, which resembles those of bulk CdSe and is also affected by TOPSe ligand. However, Se atoms' chemical status underwent a change as the initial TOP ligands that bound to Cd atoms in the form of TOP-Se-CdSe QD were removed by S^{2-}, leaving its binding type dominated by the Se−Cd bond and thus giving a BE value of around 54.3 eV, which is close to that of bulk CdSe.[48,51] Removal of the TOPSe was also verified by EDS spectra in which a considerable loss of the Se element can be observed. Therefore, our XPS observations are supportive to a certain degree of the hypothesis that the sulfur ions were introduced onto the surface of QDs by forming the −S−Cd bonding type and removed the TOP ligands that were initially bound to Cd atoms to passivate the QDs.

Electron Injection into TiO_2 Films. We characterized the effect of the inorganic ligand exchange on the electron injection from the QDs to TiO_2 films using the improved TG technique. At first, we confirmed the dependence of the TG responses on the pump intensity (from 2 to 20 μJ/pulse). The decay of the TG responses becomes faster as the pump intensity increases when the pump intensity is larger than 4 μJ/pulse, which can be considered to result from an Auger recombination (Supporting Information Figure S7). Yet we found that the dependence of the maximum signal intensity on the pump intensity was linear, and the waveforms of the responses overlapped with each other very well when they were normalized at the peak intensity for the pump intensity smaller than 4 μJ/pulse (Supporting Information Figure S7). So, in our experiments, the TG responses were measured with pump intensity of 2 μJ/pulse for all samples. Thus, two-body and three-body recombination processes could be neglected under this condition. Therefore, it is reasonable to assume that the depopulation dynamics of the photoexcited electrons and holes in the CdSe QDs measured in the TG response are due to one-body recombination processes such as trapping and transfer under our experimental conditions in this study.

Figure 5 shows TG responses of CdSe QDs-sensitized TiO_2 films with (a) TOP organic ligand capped-CdSe QDs and (b)

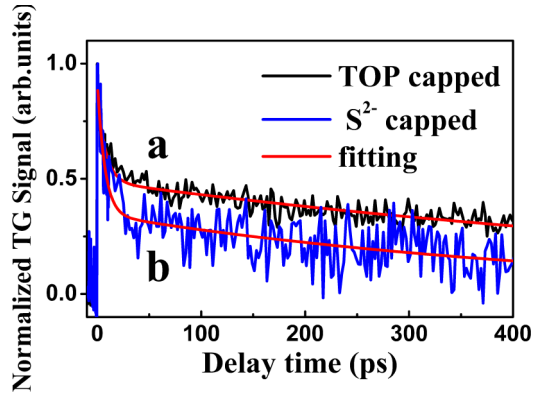

Figure 5. Normalized TG responses of TiO_2 films adsorbed with CdSe QDs capped with (a) typical organic ligand TOP and (b) inorganic ligand S^{2-}. The measurements were carried out in N_2 environment.

S^{2-} inorganic ligand capped-CdSe QDs, which were measured in N_2 atmosphere. The TG signal $S(t)$ in the fast time scale used in this study (less than nanosecond) is proportional to a change in the refractive index of the samples resulted from photoexcited carriers. As studied in detail in previous papers, it is known that the change in the refractive index $\Delta n(t)$ for semiconductor QDs as a function of time t can be expressed approximately with a modified Drude theory as follows:[28−38,52,53]

$$\Delta n(t) = \Gamma A\left(\frac{-N_e(t)}{m_e} + \frac{-N_h(t)}{m_h}\right) \quad (1)$$

where the first and second terms are the refraction changes induced by photoexcited electrons and holes, respectively. $N_e(t)$ and $N_h(t)$ are the photoexcited electron and hole densities, respectively. m_e and m_h are the effective masses of electrons and holes, respectively. A is a constant for a given probe beam wavelength, and Γ is the optical confinement factor in the QDs.[53]

As shown in eq 1, the important feature of the TG signal is that both photoexcited electron and hole carriers in the samples contribute to the signal. The exact contribution from each type of carrier depends inversely on its carrier effective mass. According to the Drude theory, we can consider that only photoexcited electrons and holes are responsible for the population grating signals. Basically, the surface state traps represent localized states that are off-resonance from the probe. The subsequent change in optical properties of surface trap sites, at the probe wavelengths used, is at least an order of magnitude smaller than that of free carrier popution grating.[34−38,52] So we suppose that the TG decay provides a direct measurement of free electron and hole carrier population dynamics and is irrespective of the trapped electrons and holes.[34−38,52] For CdSe, the effective masses of holes and electron are $0.44m_0$ and $0.13m_0$ (m_0 is the electron rest mass), respectively,[54] so both the photoexcited electron and hole carrier densities in the CdSe QDs contribute to the signal. It is known that the effective mass of electron of TiO_2 is about $30m_0$,[52] which is much larger than that of the CdSe. Therefore,

dx.doi.org/10.1021/jp410599q | J. Phys. Chem. C 2014, 118, 214−222

the TG signal due to the transferred electrons in TiO_2 can be ignored in this case for the fast time scale.

We found that the TG response shown in Figure 5 could be fitted very well with a biexponential decay function as shown in eq 2:

$$y = A_1 e^{-t/\tau_1} + A_2 e^{-t/\tau_2} \quad (2)$$

where A_1 and A_2 are constants, and τ_1 and τ_2 are time constants of two decay process. The fitting results (time constants of the fast (τ_1) and slow (τ_2) decay processes and the corresponding A_1 and A_2 (the components of the two decay)) are summarized in Table 3.

Table 3. Fitting Results of the TG Responses of CdSe QD-Sensitized TiO_2 Films Shown in Figure 5 with a Double Exponential Decay Equation (Eq 2), Where the CdSe QDs Were Capped with Typical Organic Ligand TOP and Inorganic Ligand S^{2-}[a]

sample	τ_1 (ps)	τ_2 (ps)	A_1	A_2
TOP capped	8.6 ± 0.7	827 ± 47	0.37 ± 0.01	0.52 ± 0.01
S^{2-} capped	7.1 ± 0.9	455 ± 54	0.58 ± 0.07	0.35 ± 0.02

[a] τ_1 and τ_2 are time constants; A_1 and A_2 are constants.

Through characterization of CdSe-sensitized rutile single crystals by means of AFM,[24,34] it is known that the direct adsorption of QDs favors a random mechanism of adsorption, leading to aggregation rather than to homogeneous monolayer adsorption. So electron injections occur from the QDs directly adsorbed on TiO_2 film and also those not directly adsorbed on TiO_2 film. As discussed in detail in previous papers,[34,35,37,38] for the QDs-sensitized films prepared with the direct adsorption method as used in this study, the fast decay process in the TG response relates to hole trapping and fast electron injection from the QDs directly adsorbed on TiO_2 (first monolayer), while the slow decay process relates to slower electron injection from QDs that are not directly adsorbed on TiO_2. According to the values of the effective masses, the contribution to TG signal from holes is about 30% of that from electrons in CdSe.[34] Paying attention to the amplitude coefficients A_1 and A_2 in Table 3, we observe that the A_1/A_2 value is larger than 30%. This strongly supports the consideration that the fast decay is largely attributed to fast electron injection besides holes trapping. As shown in Table 3, after ligand exchange from TOP to S^{2-} in the QD-sensitized film, the fast decay time decreased from 8.6 to 7.1 ps, and the slow decay time decreased greatly from 827 to 455 ps. In addition, the A_1/A_2 value increases from 0.64 to 1.6. These results indicate that electron injection in CdSe QDSSCs became much faster after ligand exchange from TOP to S^{2-} on the surface of the CdSe QDs. As discussed in a previous paper,[34] assuming that such an electron transfer process takes place by tunnelling from the excited QD to TiO_2,[34] the distance and the properties of the ligands between the QDs and TiO_2 film and between the QDs and QDs are key parameters controlling the rate of injection. So, our experimental results mean that inorganic S^{2-} ligand exchange on CdSe QDs can improve the electron injection rate greatly as compared to TOP ligands. This can be considered to be due to a CdS monolayer produced on the CdSe QDs after the ligand exchange, which can result in shorter distances between QDs and TiO_2 and between QDs and QDs as compared to TOP ligand. The faster electron injection can provide a higher IPCE value and a higher short circuit current in the case of S^{2-} capping. In fact, this has been demonstrated and will be shown in the following sections.

DEVICE PERFORMANCE

Obviously, from what we have discussed above, one can safely draw the conclusion that the S^{2-} treatment of CdSe-sensitized TiO_2 films has led to a significant inorganic ligand exchange of QDs. Next, we evaluate the influence that this kind of ligand exchange would bring on the performance of the CdSe QDSSCs. The sensitized photoanodes based on 3.5 nm CdSe QDs, 72 h for QDs' adsorption onto TiO_2 mesoporous films, and 46 h for S^{2-} treatment were employed to fabricate the QDSSCs.

IPCE Results and *J*–*V* Curves. The IPCE spectra recorded at different incident light wavelengths for TOP capped and S^{2-} capped solar cell are shown in Figure 6. The spectra clearly

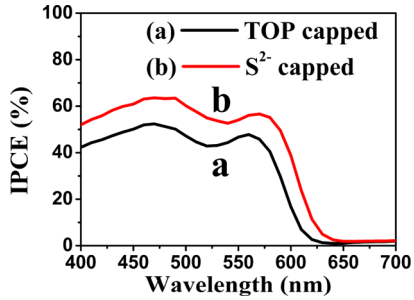

Figure 6. Comparison of IPCE spectra of CdSe QDSSCs before and after S^{2-} ligand exchange.

show that the overall photocurrent response parallels the QD/TiO_2 film absorption features with photocurrent onsets around 600 and 620 nm before and after inorganic ligand exchange, respectively. Significant improvement in IPCE value in the whole absorption wavelength range is observed for the S^{2-} capped solar cell with the maximum IPCE in the range of 50–65%, evidencing more efficient electrons transfer from QDs to TiO_2 matrix and holes toward electrolyte, as well as showing the benefits of introducing S^{2-} onto the surface of QDs in providing a better electronic transmission path. We consider the enhanced IPCE value of the inorganic ligand passivated device to arise from the modified short-range interparticles' communication between QDs and TiO_2 for electron injection. It is believed that the almost insulating organic molecules would create a spatial separation between QD electron donors and wide gap semiconductor electron acceptors, reducing electron tunneling injection and thus reducing the photocurrent obtained.[55] Therefore, the absence of the insulating TOP organic layers can be helpful to shorten the electron transfer distance, enhancing short-range interparticles' communication between nanoparticles. What is more, removal of the initial TOP passivants may also bring a positive effect on promoting the access of the aqueous electrolyte penetrating into the TiO_2 pores and leading to intimate contact between electrolyte and QDs when we take into account the hydrophobic characteristic of the organic TOP chains. These considerations can be supported strongly by the observation of the increase of electron injection rate after S^{2-} ligands exchange from TOP ligands as mentioned above.

The *J*–*V* characteristics of QDSSCs employing organic and inorganic capping ligands are presented, respectively, in Figure

dx.doi.org/10.1021/jp410599q | J. Phys. Chem. C 2014, 118, 214–222

7. The detailed photovoltaic parameters are shown in Table 4. An impressive enhancement in three parameters can be seen in

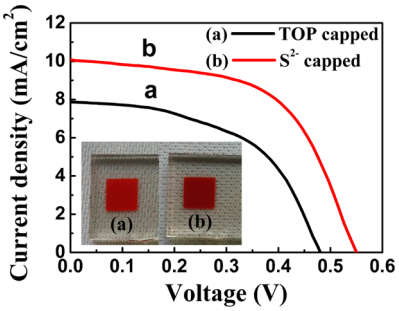

Figure 7. $J-V$ characteristics of CdSe QDSSCs under AM 1.5 with (a) typical organic ligand capped CdSe QDs-sensitized TiO_2 films and (b) S^{2-} capped CdSe QDs-sensitized TiO_2 films.

Table 4. Photovoltaics Parameters of CdSe QDSSCs with TOP Ligands and with S^{2-} Ligands

device	V_{oc} (V)	J_{sc} (mA/cm^2)	FF (%)	η (%)
TOP capped	0.47	7.85	52.31	1.92
S^{2-} capped	0.55	10.11	57.16	3.17

S^{2-} capped device as compared to the TOP capped one, resulting in the overall efficiency of 3.17%, an inspiring PCE performance for the as-synthesized CdSe QDSSCs. Yet the PCE was much lower than that of the typical dye-sensitized solar cells, which we consider to be limited by the intrinsic property of QDs, with an insufficient amount of the QDs on TiO_2 network and nanometric barriers between QDs and electrolyte. The open circuit voltage of 0.55 V and fill factor of 0.57 were achieved with the inorganic ligands, allowing this kind of cell to be comparable to that of SILAR prepared cells.[56,57] A 29% improvement in short circuit current can be seen in S^{2-} capped cell, consistent with the increase in IPCE value. However, the J_{sc} value was still lag behind of those SILAR prepared ones, implying insufficient QDs' loading on the oxide matrix for light harvesting in the present ex situ method prepared cells.

EIS Discussion. To intuitively display the origin of the enhanced photocurrent and photovoltage after S^{2-} ligand exchange, electrochemical impedance spectroscopy (EIS) was carried out to study the interfacial behavior of the photoexcited electrons. Figure 8 shows the EIS spectra of the CdSe QDSSCs

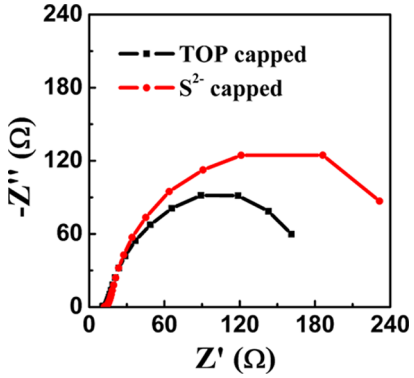

Figure 8. EIS spectra of CdSe QDSSCs with TOP and S^{2-} ligand capped.

before and after S^{2-} ligand exchange in the dark under a forward bias of −0.6 V with a frequency ranging from 0.08 Hz to 1000 kHz. The radius of the semicircle in the middle-frequency area corresponding to the electron transfer resistance at the photoanode/electrolyte interface, as we can see from Figure 8, is larger in the case of S^{2-} ligand capped film, indicating that the inorganic passivation scheme effectively increases the interface recombination resistance between the electron that has been injected to TiO_2 and QDs/electrolyte. What is more, the result further displays an improved connection between CdSe QDs and TiO_2, which is helpful for the injection of the photoexcited electrons.

Influence of S^{2-} Treatment on SILAR Method. We have also investigated the impact of S^{2-} treatment on CdSe QDs deposited on TiO_2 films by the in situ method (SILAR) (Supporting Information 7), and it turned out that the PCE did not show an obvious change after this S^{2-} treatment. In situ prepared CdSe QDs on TiO_2 films are free of organic ligands, allowing naturally tight contact between QDs and TiO_2, while the S^{2-} treatment is helping to remove the organic ligands in the case of the ex situ method, which is the reason this treatment can play a positive role in improving ex situ PCE but faded in the in situ case.

CONCLUSIONS

We have presented a simple way to boost the performance of the as-synthesized CdSe QDSSCs by introducing the inorganic ions to passivate the QDs' surface. Electron injection from CdSe QDs to TiO_2 nanoparticles became much faster, and charge recombination was largely suppressed in the case of S^{2-} capping as a result of the modified nanoparticles' communication and well-passivated surface states. We first employed these inorganic passivation CdSe QDs-sensitized films to fabricate QDSSCs with the efficiency of 3.17%, a 65% enhancement in the power conversion efficiency as compared to that of the organic ligands-capped cells. Further improvement can be expected if the original TOP ligands substituted completely by inorganic ligands and a considerable amount of the inorganic ligands-capped CdSe submonolayer coverage was achieved on the nanoporous TiO_2 network. Further work is in progress.

ASSOCIATED CONTENT

Supporting Information

Optical property and TEM image of CdSe QDs in solvent, additional information on QDs' adsorption to mesoporous TiO_2 films, XRD patterns and FT-IR spectra, details on ruling out the influence that S^{2-} treatment brings on changing the property of TiO_2 nanoparticles, TG responses, experimental procedures for CdSe QDs prepared by SILAR, and its treatment. This material is available free of charge via the Internet at http://pubs.acs.org.

AUTHOR INFORMATION

Corresponding Authors

*Tel.: +86 0551-65593222. E-mail: zhujzhu@gmail.com.
*Tel.: +81 424435464. E-mail: shen@pc.uec.ac.jp.
*Tel.: +86 0551-65591377. E-mail: sydai@ipp.ac.cn.

Notes

The authors declare no competing financial interest.

■ ACKNOWLEDGMENTS

This work was supported by the National Basic Research Program of China under Grant No. 2011CBA00700, the National High Technology Research and Development Program of China under Grant No. 2011AA050527, the External Cooperation Program of the Chinese Academy of Sciences under Grant No. GJHZ1220, the Program of Hefei Center for Physical Science and Technology (2012FXZY006), and the National Natural Science Foundation of China under Grant Nos. 21173228, 61204075. Q.S. and T.T. are thankful for the support by the CREST program of the Japan Science and Technology Agency (JST).

■ REFERENCES

(1) Ruhle, S.; Shalom, M.; Zaban, A. Quantum-Dot-Sensitized Solar Cells. *ChemPhysChem* **2010**, *11*, 2290−2304.
(2) Talapin, D. V.; Lee, J. S.; Kovalenko, M. V.; Shevchenko, E. V. Prospects of Colloidal Nanocrystals for Electronic and Optoelectronic Applications. *Chem. Rev.* **2010**, *110*, 389−458.
(3) Kamat, P. V. Quantum Dot Solar Cells. Semiconductor Nanocrystals as Light Harvesters. *J. Phys. Chem. C* **2008**, *112*, 18737−18753.
(4) Lee, H.; Leventis, H. C.; Moon, S.-J.; Chen, P.; Ito, S.; Haque, S. A.; Torres, T.; Nüesch, F.; Geiger, T.; Zakeeruddin, S. M.; et al. PbS and CdS Quantum Dot-Sensitized Solid-State Solar Cells: "Old Concepts, New Results". *Adv. Funct. Mater.* **2009**, *19*, 2735−2742.
(5) Peter, L. M.; Riley, D. J.; Tull, E. J.; Wijayantha, K. G. U. Photosensitization of Nanocrystalline TiO_2 by Self-Assembled Layers of CdS Quantum Dots. *Chem. Commun.* **2002**, *38*, 1030−1031.
(6) Shen, Q.; Sato, T.; Hashimoto, M.; Chen, C. C.; Toyoda, T. Photoacoustic and Photoelectrochemical Characterization of CdSe-Sensitized TiO_2 Electrodes Composed of Nanotubes and Nanowires. *Thin Solid Films* **2006**, *499*, 299−305.
(7) Plass, R.; Pelet, S.; Krueger, J.; Gratzel, M.; Bach, U. Quantum Dot Sensitization of Organic-Inorganic Hybrid Solar Cells. *J. Phys. Chem. B* **2002**, *106*, 7578−7580.
(8) Luther, J. M.; Beard, M. C.; Song, Q.; Law, M.; Ellingson, R. J.; Nozik, A. J. Multiple Exciton Generation in Films of Electronically Coupled PbSe Quantum Dots. *Nano Lett.* **2007**, *7*, 1779−1784.
(9) Chang, J. A.; Im, S. H.; Lee, Y. H.; Kim, H.-j.; Lim, C.-S.; Heo, J. H.; Seok, S. I. Panchromatic Photon-Harvesting by Hole-Conducting Materials in Inorganic-Organic Heterojunction Sensitized-Solar Cell through the Formation of Nanostructured Electron Channels. *Nano Lett.* **2012**, *12*, 1863−1867.
(10) Kojima, A.; Teshima, K.; Shirai, Y.; Miyasaka, T. Organometal Halide Perovskites as Visible-Light Sensitizers for Photovoltaic Cells. *J. Am. Chem. Soc.* **2009**, *131*, 6050−6051.
(11) Im, J. H.; Lee, C. R.; Lee, J. W.; Park, S. W.; Park, N. G. 6.5% Efficient Perovskite Quantum-Dot-Sensitized Solar Cell. *Nanoscale* **2011**, *3*, 4088−4093.
(12) Lee, H. J.; Yum, J. H.; Leventis, H. C.; Zakeeruddin, S. M.; Haque, S. A.; Chen, P.; Seok, S. I.; Grazel, M.; Nazeeruddin, M. K. CdSe Quantum Dot-Sensitized Solar Cells Exceeding Efficiency 1% at Full-Sun Intensity. *J. Phys. Chem. C* **2008**, *112*, 11600−11608.
(13) Zhang, H.; Cheng, K.; Hou, Y. M.; Fang, Z.; Pan, Z. X.; Wu, W. J.; Hua, J. L.; Zhong, X. H. Efficient CdSe Quantum Dot-Sensitized Solar Cells Prepared by a Postsynthesis Assembly Approach. *Chem. Commun.* **2012**, *48*, 11235−11237.
(14) Pan, Z. X.; Zhang, H.; Cheng, K.; Hou, Y. M.; Hua, J. L.; Zhong, X. H. Highly Efficient Inverted Type-I CdS/CdSe Core/Shell Structure QD-Sensitized Solar Cells. *ACS Nano* **2012**, *6*, 3982−3991.
(15) Pan, Z.; Zhao, K.; Wang, J.; Zhang, H.; Feng, Y.; Zhong, X. Near Infrared Absorption of $CdSe_xTe_{1-x}$ Alloyed Quantum Dot Sensitized Solar Cells with More than 6% Efficiency and High Stability. *ACS Nano* **2013**, *7*, 5215−5222.
(16) Wang, J.; Mora-Seró, I.; Pan, Z.; Zhao, K.; Zhang, H.; Feng, Y.; Yang, G.; Zhong, X.; Bisquert, J. Core/Shell Colloidal Quantum Dot Exciplex States for the Development of Highly Efficient Quantum-Dot-Sensitized Solar Cells. *J. Am. Chem. Soc.* **2013**, *135*, 15913−15922.
(17) Ip, A. H.; Thon, S. M.; Hoogland, S.; Voznyy, O.; Zhitomirsky, D.; Debnath, R.; Levina, L.; Rollny, L. R.; Carey, G. H.; Fischer, A.; et al. Hybrid Passivated Colloidal Quantum Dot Solids. *Nat. Nanotechnol.* **2012**, *7*, 577−582.
(18) Tang, J.; Kemp, K. W.; Hoogland, S.; Jeong, K. S.; Liu, H.; Levina, L.; Furukawa, M.; Wang, X. H.; Debnath, R.; Cha, D. K.; et al. Colloidal-Quantum-Dot Photovoltaics Using Atomic-Ligand Passivation. *Nat. Mater.* **2011**, *10*, 765−771.
(19) Ning, Z. J.; Ren, Y.; Hoogland, S.; Voznyy, O.; Levina, L.; Stadler, P.; Lan, X. Z.; Zhitomirsky, D.; Sargent, E. H. All-Inorganic Colloidal Quantum Dot Photovoltaics Employing Solution-Phase Halide Passivation. *Adv. Mater.* **2012**, *24*, 6295−6299.
(20) Niu, G. D.; Wang, L. D.; Gao, R.; Ma, B. B.; Dong, H. P.; Qiu, Y. Inorganic Iodide Ligands in Ex Situ PbS Quantum Dot Sensitized Solar Cells with I^-/I_3^- Electrolytes. *J. Mater. Chem.* **2012**, *22*, 16914−16919.
(21) de la Fuente, M. S.; Sanchez, R. S.; Gonzalez-Pedro, V.; Boix, P. P.; Mhaisalkar, S. G.; Rincon, M. E.; Bisquert, J.; Mora-Sero, I. Effect of Organic and Inorganic Passivation in Quantum-Dot-Sensitized Solar Cells. *J. Phys. Chem. Lett.* **2013**, *4*, 1519−1525.
(22) Chen, O.; Chen, X.; Yang, Y.; Lynch, J.; Wu, H.; Zhuang, J.; Cao, Y. C. Synthesis of Metal-Selenide Nanocrystals Using Selenium Dioxide as the Selenium Precursor. *Angew. Chem., Int. Ed.* **2008**, *47*, 8638−8641.
(23) Wang, Q.; Pan, D. C.; Jiang, S. C.; Ji, X. L.; An, L. J.; Jiang, B. Z. A Solvothermal Route to Size- and Shape-Controlled CdSe and CdTe Nanocrystals. *J. Cryst. Growth* **2006**, *286*, 83−90.
(24) Guijarro, N.; Lana-Villarreal, T.; Mora-Sero, I.; Bisquert, J.; Gomez, R. CdSe Quantum Dot-Sensitized TiO_2 Electrodes: Effect of Quantum Dot Coverage and Mode of Attachment. *J. Phys. Chem. C* **2009**, *113*, 4208−4214.
(25) Gimenez, S.; Mora-Sero, I.; Macor, L.; Guijarro, N.; Lana-Villarreal, T.; Gomez, R.; Diguna, L. J.; Shen, Q.; Toyoda, T.; Bisquert, J. Improving the Performance of Colloidal Quantum-Dot-Sensitized Solar Cells. *Nanotechnology* **2009**, *20*, 295204(1−6).
(26) Hu, L. H.; Dai, S. Y.; Weng, J.; Xiao, S. F.; Sui, Y. F.; Huang, Y.; Chen, S. H.; Kong, F. T.; Pan, X.; Liang, L. Y.; et al. Microstructure Design of Nanoporous TiO_2 Photoelectrodes for Dye-Sensitized Solar Cell Modules. *J. Phys. Chem. B* **2007**, *111*, 358−362.
(27) Hodes, G.; Manassen, J.; Cahen, D. Electrocatalytic Electrodes for the Polysulfide Redox System. *J. Electrochem. Soc.* **1980**, *127*, 544−549.
(28) Katayama, K.; Yamaguchi, M.; Sawada, T. Lens-Free Heterodyne Detection for Transient Grating Experiments. *Appl. Phys. Lett.* **2003**, *82*, 2775−2777.
(29) Shen, Q.; Katayama, K.; Yamaguchi, M.; Sawada, T.; Toyoda, T. Study of Ultrafast Carrier Dynamics of Nanostructured TiO_2 Films with and without CdSe Quantum Dot Deposition Using Lens-Free Heterodyne Detection Transient Grating Technique. *Thin Solid Films* **2005**, *486*, 15−19.
(30) Diguna, L. J.; Shen, Q.; Sato, A.; Katayama, K.; Sawada, T.; Toyoda, T. Optical Absorption and Ultrafast Carrier Dynamics Characterization of CdSe Quantum Dots Deposited on Different Morphologies of Nanostructured TiO_2 Films. *Mater. Sci. Eng., C* **2007**, *27*, 1514−1520.
(31) Shen, Q.; Yanai, M.; Katayama, K.; Sawada, T.; Toyoda, T. Optical Absorption, Photosensitization, and Ultrafast Carrier Dynamic Investigations of CdSe Quantum Dots Grafted onto Nanostructured SnO_2 Electrode and Fluorine-Doped Tin Oxide (FTO) Glass. *Chem. Phys. Lett.* **2007**, *442*, 89−96.
(32) Shen, Q.; Katayama, K.; Sawada, T.; Toyoda, T. Characterization of Electron Transfer from CdSe Quantum Dots to Nanostructured TiO_2 Electrode Using a Near-Field Heterodyne Transient Grating Technique. *Thin Solid Films* **2008**, *516*, 5927−5930.
(33) Shen, Q.; Ayuzawa, Y.; Katayama, K.; Sawada, T.; Toyoda, T. Separation of Ultrafast Photoexcited Electron and Hole Dynamics in

CdSe Quantum Dots Adsorbed onto Nanostructured TiO_2 Films. *Appl. Phys. Lett.* **2010**, *97*, 263113−263113−3.
(34) Guijarro, N.; Shen, Q.; Gimenez, S.; Mora-Sero, I.; Bisquert, J.; Lana-Villarreal, T.; Toyoda, T.; Gomez, R. Direct Correlation between Ultrafast Injection and Photoanode Performance in Quantum Dot Sensitized Solar Cells. *J. Phys. Chem. C* **2010**, *114*, 22352−22360.
(35) Guijarro, N.; Lana-Villarreal, T.; Shen, Q.; Toyoda, T.; Gomez, R. Sensitization of Titanium Dioxide Photoanodes with Cadmium Selenide Quantum Dots Prepared by SILAR: Photoelectrochemical and Carrier Dynamics Studies. *J. Phys. Chem. C* **2010**, *114*, 21928−21937.
(36) Shen, Q.; Katayama, K.; Sawada, T.; Hachiya, S.; Toyoda, T. Ultrafast Carrier Dynamics in PbS Quantum Dots. *Chem. Phys. Lett.* **2012**, *542*, 89−93.
(37) Gonzalez-Pedro, V.; Shen, Q.; Jovanovski, V.; Gimenez, S.; Tena-Zaera, R.; Toyoda, T.; Mora-Sero, I. Ultrafast Characterization of the Electron Injection from CdSe Quantum Dots and Dye N719 Co-Sensitizers into TiO_2 Using Sulfide Based Ionic Liquid for Enhanced Long Term Stability. *Electrochim. Acta* **2013**, *100*, 35−43.
(38) Gonzalez-Pedro, V.; Sima, C.; Marzari, G.; Boix, P. P.; Gimenez, S.; Shen, Q.; Dittrich, T.; Mora-Sero, I. High Performance PbS Quantum Dot Sensitized Solar Cells Exceeding 4% Efficiency: The Role of Metal Precursors in the Electron Injection and Charge Separation. *Phys. Chem. Chem. Phys.* **2013**, *15*, 13835−13843.
(39) Yu, W. W.; Qu, L. H.; Guo, W. Z.; Peng, X. G. Experimental Determination of the Extinction Coefficient of CdTe, CdSe, and CdS Nanocrystals. *Chem. Mater.* **2003**, *15*, 2854−2860.
(40) Chakrapani, V.; Baker, D.; Kamat, P. V. Understanding the Role of the Sulfide Redox Couple (S^{2-}/S_n^{2-}) in Quantum Dot-Sensitized Solar Cells. *J. Am. Chem. Soc.* **2011**, *133*, 9607−9615.
(41) Koole, R.; Luigjes, B.; Tachiya, M.; Pool, R.; Vlugt, T. J. H.; Donega, C. D. M.; Meijerink, A.; Vanmaekelbergh, D. Differences in Cross-Link Chemistry between Rigid and Flexible Dithiol Molecules Revealed by Optical Studies of CdTe Quantum Dots. *J. Phys. Chem. C* **2007**, *111*, 11208−11215.
(42) Talapin, D. V.; Rogach, A. L.; Kornowski, A.; Haase, M.; Weller, H. Highly Luminescent Monodisperse CdSe and CdSe/ZnS Nanocrystals Synthesized in a Hexadecylamine-Trioctylphosphine Oxide-Trioctylphospine Mixture. *Nano Lett.* **2001**, *1*, 207−211.
(43) Nag, A.; Kovalenko, M. V.; Lee, J. S.; Liu, W. Y.; Spokoyny, B.; Talapin, D. V. Metal-free Inorganic Ligands for Colloidal Nanocrystals: S^{2-}, HS^-, Se^{2-}, HSe^-, Te^{2-}, HTe^-, TeS_3^{2-}, OH^-, and NH_2^- as Surface Ligands. *J. Am. Chem. Soc.* **2011**, *133*, 10612−10620.
(44) Morris-Cohen, A. J.; Donakowski, M. D.; Knowles, K. E.; Weiss, E. A. The Effect of a Common Purification Procedure on the Chemical Composition of the Surfaces of CdSe Quantum Dots Synthesized with Trioctylphosphine Oxide. *J. Phys. Chem. C* **2010**, *114*, 897−906.
(45) Rafeletos, G.; Norager, S.; O'Brien, P. Evidence for the Chemical Nature of Capping in CdSe Nanoparticles Prepared by Thermolysis in Tri-n-octylphosphine Oxide from P-Edge EXAFS Spectroscopy. *J. Mater. Chem.* **2001**, *11*, 2542−2544.
(46) Jasieniak, J.; Mulvaney, P. From Cd-Rich to Se-Rich - the Manipulation of CdSe Nanocrystal Surface Stoichiometry. *J. Am. Chem. Soc.* **2007**, *129*, 2841−2848.
(47) Kalyuzhny, G.; Murray, R. W. Ligand Effects on Optical Properties of CdSe Nanocrystals. *J. Phys. Chem. B* **2005**, *109*, 7012−7021.
(48) Katari, J. E. B.; Colvin, V. L.; Alivisatos, A. P. X-Ray Photoelectron-Spectroscopy of Cdse Nanocrystals with Applications to Studies of the Nanocrystal Surface. *J. Phys. Chem.* **1994**, *98*, 4109−4117.
(49) Young, A. G.; Green, D. P.; McQuillan, A. J. Infrared Spectroscopic Studies of Monothiol Ligand Adsorption on CdS Nanocrystal Films in Aqueous Solutions. *Langmuir* **2006**, *22*, 11106−11112.
(50) Liu, I. S.; Lo, H. H.; Chien, C. T.; Lin, Y. Y.; Chen, C. W.; Chen, Y. F.; Su, W. F.; Liou, S. C. Enhancing Photoluminescence Quenching and Photoelectric Properties of CdSe Quantum Dots with Hole Accepting Ligands. *J. Mater. Chem.* **2008**, *18*, 675−682.
(51) Du, G. H.; Liu, Z. L.; Lu, Q. H.; Xia, X.; Jia, L. H.; Yao, K. L.; Chu, Q.; Zhang, S. M. Fe_3O_4/CdSe/ZnS Magnetic Fluorescent Bifunctional Nanocomposites. *Nanotechnology* **2006**, *17*, 2850−2854.
(52) Kasinski, J. J.; Gomez-Jahn, L. A.; Faran, K. J.; Gracewski, S. M.; Miller, R. J. D. Picosecond Dynamics of Surface Electron Transfer Processes: Surface Restricted Transient Grating Studies of the N-TiO_2/H_2O Interface. *J. Chem. Phys.* **1989**, *90*, 1253.
(53) Kim, J.; Meuer, C.; Bimberg, D.; Eisenstein, G. Role of Carrier Reservoirs on the Slow Phase Recovery of Quantum Dot Semiconductor Optical Amplifiers. *Appl. Phys. Lett.* **2009**, *94*, 041112−041112-3.
(54) Yan, Y. L.; Li, Y.; Qian, X. F.; Yin, J.; Zhu, Z. K. Preparation and Characterization of CdSe Nanocrystals via Na_2SO_3-Assisted Photochemical Route. *Mater. Sci. Eng., B* **2003**, *103*, 202−206.
(55) Bakkers, E. P. A. M.; Roest, A. L.; Marsman, A. W.; Jenneskens, L. W.; de Jong-van Steensel, L. I.; Kelly, J. J.; Vanmaekelbergh, D. Characterization of Photoinduced Electron Tunneling in Gold/SAM/Q-CdSe Systems by Time-Resolved Photoelectrochemistry. *J. Phys. Chem. B* **2000**, *104*, 7266−7272.
(56) Lee, Y. L.; Lo, Y. S. Highly Efficient Quantum-Dot-Sensitized Solar Cell Based on Co-Sensitization of CdS/CdSe. *Adv. Funct. Mater.* **2009**, *19*, 604−609.
(57) Santra, P. K.; Kamat, P. V. Mn-Doped Quantum Dot Sensitized Solar Cells: A Strategy to Boost Efficiency over 5%. *J. Am. Chem. Soc.* **2012**, *134*, 2508−2511.